Innovative Biomedical Technologies and Health Care (IBTHC)

Applis Publishers

Review Article Open access

Analysis of Photodynamic Therapy Efficacy in Biomedical Systems

Jui-Teng Lin

Chairman & CEO of New Vision Inc, Taiwan and Visiting Professor at HE's University, China.

Abstract

Aim: To analyze the efficacy of photodynamic therapy (PDT) for both type-I and type–II process.

Method: Photochemical kinetic equations are solved analytically for the concentration of the photosensitizer and the oxygen, which lead to the PDT efficacy. Our nonlinear law demonstrates that the Bunsen-Roscoe reciprocity law (BRL) based on a conventional Beer-Lambert law fails in most photo biologic reaction.

Conclusion: External supply of oxygen will largely improve type-II efficacy via the enhanced ROS (in type-II). Synergistic therapy efficiency may be improved by combining PDT and PTT using nanogold and various photosensitizers.

Key words: *Photodynamic Therapy; Photosensitizers; Cancer Therapy; Ophthalmology; Corneal Cross Linking; Nonlinear Law.*

Introduction

Photodynamic therapy (PDT) and photothermal therapy (PTT) have been widely used in various biomedical systems for healthy cares such as: dermatology surgery, dentistry, cancer therapy [1-3], andophthalmology applications for vision corrections and corneal deceases [4, 5]. Enhancement of PDT efficacy has been reported by combining nanoparticles [6-14]. Medical laser applications including the laser spectra of UV (200-400) um, visible (400-700) nm, near-IR (700-2900) nm, and mid-IR (3-5) um having various penetration depths which define invasive and noninvasive procedures have been reviewed recently [15]. This review article will focus on the applications of photodynamic therapy (PDT) in various biomedical systems including cancer therapy and the treatment of corneal diseases, where type-I and type-II processes will be discussed in great details.

The prior work for the modeling of PDT efficacy by Zhu et al. [16], Schumacher et al. [17], and Kling [18] assumed a constant light intensity and ignored the photosensitizer depletion based on the conventional Beer-Lambert law which underestimated the UV light intensity. The prior work also assumed a flat photo sensitizer concentration and ignored the absorption of the photolytic products. This study will remove the above described over simplified assumptions for a much more realistic and accurate prediction of the key parameters influencing the PDT efficacy. A generalized, time-dependent Beer-Lambert law is employed to solve the dynamic light intensity [19]. The role of oxygen for improvement of the type-II efficacy via the enhanced reactive oxygen species (ROS) will be discussed [20]. Synergistic therapy efficiency may be improved by combining PDT and PTT using nanogold and various photosensitizers is analyzed [21-25].

The Applications of PDT

PDT offers many applications in dermatology, ophthalmology and cancer treatments in various parts of human body, including early stage (micro-invasive) lung cancer, lung tumors (endobronchial, mesothelioma), skin, brain, colorectal and breast cancer, chronic skin diseases (psoriasis, vitiligo), and oral cavity (antibacterial) [1-3, 15]. Ophthalmology applications include age-related macular degeneration (AMD), pathologic myopia induced subfocal choroidal neovascularization(CNV), coagulation of retina, and corneal crosslinking for corneal keratoconus and ulcers [4, 15]. PDT for the treatment of CNV using verteporfin as the photosensitizer has been proven for subfoveal CNV in both AMD and in pathologic myopia (or non-AMD) patients [15].

The more recent application is to use a UVA (365 nm) light to treat the corneal diseases such as corneal ulcers and keratoconus, where both type-I and type-II occur during the UV exposure of the corneal stroma diffused by riboflavin solution [4, 19]. As shown in Table 1, various photosensitizers are available for the absorption of lasers in visible (630-700) nm, and near-IR (700-1000) nm. These lasers are commercially available; dye lasers (at about 665 nm) pumped by a green laser; Nd: YAG (at 1064 nm); diode lasers (630-1100) nm; tunable Ti:sapphire laser (690-1100) nm; Alexandrite laser (720-800) nm. Tunable near-IR source may be also generated from an optical parametric oscillation (OPO) or amplification (OPA), where a green laser (at about 532 nm) may be used as a pump to produce tunable (900-1300) nm near-IR output. In addition, high-brightness LED in visible (550-680) nm are also available for PDT using 5-ALA as the photosensitizer [15].

Kinetics of PDT

PDT involves selective light (often low-power laser light or LED) absorption by the external chemical agent (or a PDT drug). As shown in Table 1, various dyes (drugs) have been developed at specific laser absorption wavelengths from visible to near-IR. The PDT drugs may be administered either intravenously or topically depending on applications. Three principal mechanisms have been proposed for the destruction of cells and tissues by PDT: (a) localized cell damage by targeting on a specific organelle by a particular drugs, including apoptosis (localized in mitochondiria) and necrosis (localized in

***Address for Correspondence:** Jui-Teng Lin, Chairman & CEO of New Vision Inc, Taipei, Taiwan, E-Mail: jtlin55@gmail.com

Received: June 5, 2017; **Accepted:** June 28, 2017; **Published:** June 30, 2017

plasma membrane); (b) vascular damage induced by PDT action. For example, the porphyrin-induced PDT produces a rapid onset of vasccular blood flow stasis (stopping) and hemorrhage causing tumor cell death; and (c) immunological response of PDT results a strong inflammatory reaction which contributes to tumor destruction.

Table 1. Summary of photosensitizers [14]

Absorbing	Extinction wavelength (nm)	Coeff. 1/M/cm)
Name of PDT drug		
Riboflavin (B2)	365, 430 470 (%/cm)	--
Photofrin (porfimer sodium)	630	3,000
5-ALA	635	5,000
Meta-THPC	652	22,400
Methylene blue	630, 660	--
pyropheophorbides (HPPH)	665	--
verteporfin	680-690	--
Lu-Tex	732	42,000
Phthalocyanines , na-PTC	670-780	100,000
Indocyanin green (ICG)	780-850	--
Si(IV)-naphthalocyanines	770-790	240,000

The photochemical process of PDT further involves 2 chemical processes [17]:

a) Photoaddition reaction (type-I) in which the light-excited photosensitizer covalently bonds to a constituent molecule of the cell, where type I is the major path for crosslinking process without oxygen; and
b) Photoxidation reaction (type-II) in which the excited state of the photosensitizer produces a highly reactive oxygen specie (ROS) such as an excited singlet oxygen, a superoxide anion, or a free radical and it often involves a chain reaction, where type II is the major path for cancer cells (or bacterial) damage.

Figure 1a shows the photodynamic kinetics for UVA-activated riboflavin (RF) solution incorneas, where Rf, Rf' and Rf* are, respectively, the ground state, singlet and triplet state of RF.

Figure 1b shows the type-II PDT for cancer therapy, where S_0, S_1, S_3 are the photosensitizer concentration at ground state, singlet and triplet state; O_2 and O^* are the oxygen concentration at ground and singlet state; and [A] is the bacterial target [16, 20].

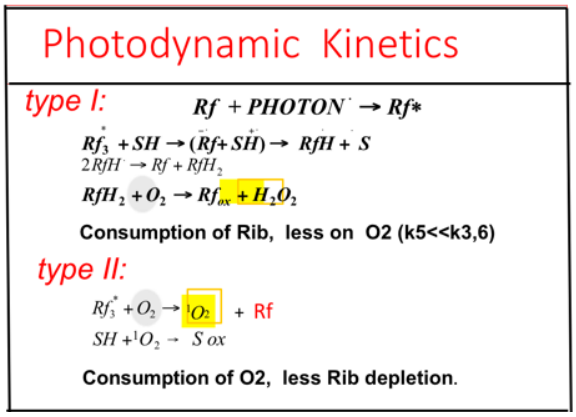

(1a)

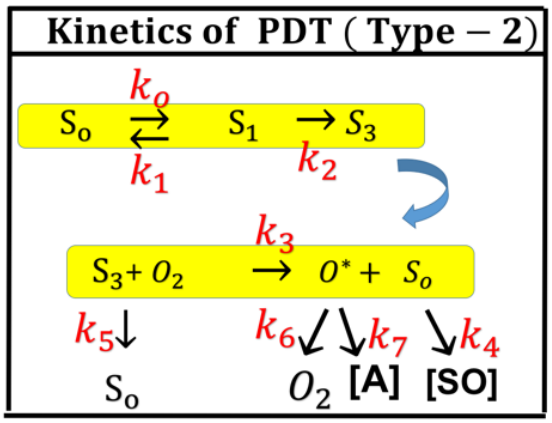

(1b)

Figure 1: The photodynamic kinetics for: (1a) UVA-activated riboflavin solution incorneal stroma; (1b) type-II PDT for cancer therapy, where [A] is the bacterial target [20].

Figure 2 shows two biomedical systems: (left) for corneal crsoolinking using UVA (365 nm), and (right) for cancer photothe-rapy, with the initial photosensitizer concentration given by C(z,0).

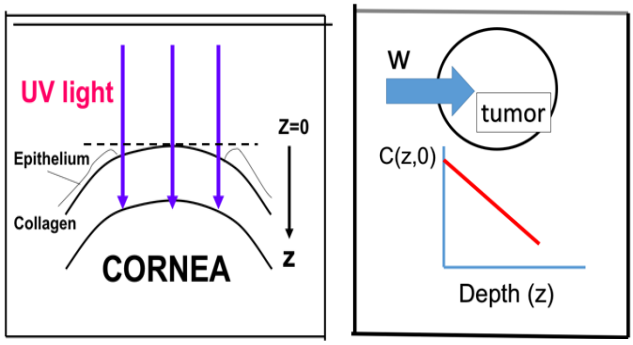

Figure 2: shows two biomedical systems: (left) for corneal crsoolinking using UVA (365 nm) and riboflavin; (right) for cancer therapy using near IR laser, with the initial photosensitizer concentration given by C(z,0).

The Efficacy of PDT

The PDT kinetic equations, in the quasi-steady-state condition [16], for the concentration of the ground state RF, C(z,t), and the ground state oxygen, X(z,t), and the singlet oxygen, X*(z,t), are given [20].

$$\frac{\partial C(z,t)}{\partial t} = -apI(z,t)\{1 + qH(z,t)]C(z,t) \quad (1.a)$$

$$\frac{\partial X}{\partial t} = -apI(z,t)H(z,t) \quad (1.b)$$

$$\frac{\partial I(z,t)}{\partial z} = -A(z,t)I(z,t) \quad (1.c)$$

where

$$A(z,t) = 2.3[(\varepsilon_1 - \varepsilon_2)X(z,t) + \varepsilon_2 X_0 F(z) + Q] \quad (2.a)$$

$$H(z,t) = C(z,t)X(z,t)/[X(z,t) + k] \quad (2/b)$$

where ε_1 and ε_2 are the extinction coefficients of RF and the photolysis product, respectively; Q is the absorption coefficient of the stroma at the UV wavelength; p and q are the type-I and type-II quantum yield, respectively, given by $p=k_2/(k_1+k_2)$ and $q=k_4/(k_7[EM])$ having a typical value 0.005 to 0.05; and $k=k_5/k_3$, having a typical value of 1.0 to 5.0 [7]. The rates constants k_j are defined in the kinetic chart shown in Figure 1, Equation (1a) has been generalized for the situation that both type-I and type-II CXL occur. It reduces to type-I only, when q=0, or dX/dt=0, or there is no oxygen supply in the process. Equation (3) has been generalized for the situation that both type-I and type-II CXL occur. It reduces to type-I only, when q=0, or dX/dt=0, or there is no oxygen supply in the process. The effective factor, defined by $f=1- (k_5+k_3X_0)/k_8[SH]$, is for the influence of type-II on the RF depletion in type-I, where the reduction of the trplet RF due to its direct coupling to the collagen substract [SH], when type-I process occurs simultaneously with type-II. This extra RF depletion term was ignored in previous modeling [16-18]. The intial concentration profile of the photosensitizer, F(z)=1-0.5z/D, and oxygen, F'(z)=1-0.5z/D', with D and D' being the diffusion depth.

Efficacy of the type-II cross linking given by the time integration of the singlet oxygenconcentration (X*). The normal-ized efficacy of type-II cross linking defined by Ceff $=1-[EM]/[EM]_0= 1-\exp(-S)$, with S-function given by [15].

$$S = k_7[EM]\int_0^t X^* \, dt \quad (3)$$

Both analytic and numerical solutions of Equations (1) and (2) have been presented by Lin [5] which, however, was limited to type-I process, with efficacy given by Ceff (I)= 1- exp(-S'), S' is a conversion factor for monomers to polymers, and having a steady state proportional to the square root of $[C_0/I_0]\exp(Az)$. We should note that the the photosensitizer concentration is depleted by the activated lightas shown by Equation. (1.a) and the conventional Beer- Lambert law, with a constant C(z,t), fails. For the case that both type-I and type-II exist, analytic formulas are also derived as follows [20].

$$S = (b/f)E_1[\,1 - b_1(1 - 0.5\,E_2/E_1)] \quad (4)$$

where

$b=(k'/f)C_0F(z)\exp(-b')$, $b'=(qk'/f)C_0F(z)E_1$,

$f=1- [k_5+k_3X_0F'(z)]/k_8[SH]$, $k'=1-k/(X_0F'(z))$,

$k=k_5/k_3$. $b_1=kb/[k'(X_0F'(z))^2]$,

$E_1=1-\exp(-Bt)$,

$E_2=1-\exp(-2Bt)$,

$B=apI(z)C_0F(z)$.

E1 and E2 are proportional to the light dose (or fluence).

Equations (1) to (4) provide us the important features for photobiology systems, summarized as follows (also referring to Figure 1):

a. PDT efficacy in type-II, Ceff (II) is an increasing function of the light dose (tI0), the photosensitizer and oxygen concentration (C0 and X0) and their diffusion depth, but it is a decreasing function to the type-II quantum yield (q), and the medium depth (z). Therefore, external supply of oxygen (with enough diffusion depth) will largely improve the type-II efficacy via the enhanced ROS. Pulsing light maybe employed to improve the continuing supply of oxygen.

b. Diffusion depth (D and D') may be enhanced by ionic RF device as being used in corneal crosslinking.

c. For improved light penetration and PDT efficacy, near IR light (laser or LED) is preferred using appropriate photosensitizers [26], where a near IR laser using upconversion to produce visible or UV laser [27-29].

d. For the same dose, longer exposure time (at lower light intensity) is more efficient than that of high intensity with shorter exposure time, where the optimal exposure time, light intensity or dose depends on the syetem conditions. So called accelerate crosslinking (by higher intensity) employed in corneas might be considered to shorten the treating time in anti-cancers.

The anti-cancer efficacy may be further improved by combining PDT and PTT using functional nanogold and various photosensitizers for cancer therapy [21-25] is shown in Figure 3. The critical factors of the synergistic therapy efficiency include: the concentration of the initiator (nanogold or photosensitizers) in the treated medium, the wavelength, energy and the irradiation period of the light applied to the medium. We should note that the two-wavelength system maybe further simplified (for commercial cost effectiveness) to a single-wavelength serving for both PDT and PTT by choosing an appropriate wavelength (such as 810 nm) which is absorbed by both nanogold (for PTT) and photosensitizers (for PDT), where either dual or single wavelength light may be employed. The single wavelength system for PTT/PDT has been reported using functional nanogolds and a cw light in near IR [21-25]. The temperature increase in PTT process has been reported with various novel techniques (focusing light or pulsing mode) for improved efficacy for cancer cells killing [14, 30-32].

Conclusion

We have presented the formulas for the PDT efficacy. Our non-linear law demonstrates that the BRL restricted to a narrow limit for most photo biologic reaction. External supply of oxygen will largely improve type-II efficacy via the enhanced ROS. Synergistic therapy efficiency maybe improved by combining PDT and PTT using funct-ional nanogold and various photosensitizers.

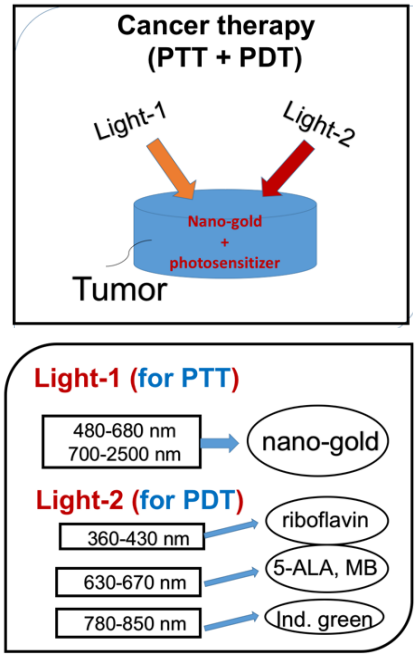

Figure 3: Combining PDT and PTT uisng nano gold and various photo sensitizers [14].

References

1. Abdel-Kader MH. Photodynamic therapy: from theory to application. Heidelberg. Springer. 2014. [Crossref]
2. Maranda EL, Nguyen AH, Lim VM, Hafeez F and Jimenez JJ. Laser and light therapies for the treatment of nail psoriasis. J Eur Acad Dermatol Venereol. 2016; 30:1278-1284. [Crossref]
3. Schelle FI, Polz S, Haloui H, Braun A, Dehn C, Frentzen M, et al. Ultrashort pulsed laser (USPL) application in dentistry: basic investigations of ablation rates and thresholds on oral hard tissue and restorative materials. J Lasers Med Sci. 2014; 29:1775-1783. [Crossref]
4. Hafezi F and Randleman JB. editors. Corneal Collagen Cross-linking, second ed. Thorofare (NJ): SLACK; 2017. [Crossref]
5. Lin JT. Combined analysis of safety and optimal efficacy in UV-light-activated corneal collagen crosslinking. Ophthalmology Research. 2016; 6:1-14. [Crossref]
6. Klein JW, van Driel PB, Snoeks TJ, Prokopi N, Fransen MF, Cruz LJ, et al. Combination of photodynamic therapy and specific immunotherapy efficiently eradicates established tumors. Clin Cancer Res. 2016; 22:1459-1468. [Crossref]
7. Inoue K. 5-Aminolevulinic acid-mediated photodynamic therapy for bladder cancer. Int J Urol. 2017; 24:97-101. [Crossref]
8. Walther J, Schastak S, Dukic-Stefanovic S, Wiedemann P, Neuhaus J and Claudep-ierre T. Efficient photodynamic therapy on human retinoblastoma cell lines. PLoS One. 2014; 9:e87453. [Crossref]
9. Tudor D, Nenu I, Filip GA, Olteanu D, Cenariu M, Tabaran F, et al. Combined regimen of photodynamic therapy mediated by gallium phthalocyanine chloride and metformin enhances anti-melanoma efficacy. PLoS One. 2017; 12:e0173241. [Crossref]
10. Chang K, Liu Z, Xiaofeng Fang, Haobin Chen, Xiaoju Men, Ye Yuan, et al. Enhanced phototherapy by nanoparticle-enzyme via generation and photolysis of hydrogen peroxide. Nanolett. 2017. [Crossref]
11. Cai Y, Tang Q, Wu X, Weili Si, Qi Zhang, Wei Huang, et al. Bromo-substituted Diketopyrrolopyrrole Derivative with Specific Targeting and High Efficiency for Photodynamic Therapy. ACS Appl Mater Interfaces. 2016; 8:10737-10742. [Crossref]
12. Lin JT, Hong YL, Chang CL. Selective cancer therapy via IR-laser-excited gold nanorods. Proc. SPIE. 2010. [Crossref]
13. Huang XH, El-Sayed IH, Qian W and El-Sayed MA. Cancer cells assemble and align gold nanorods conjugated to antibodies to produce highly enhanced, sharp, and polarized surface Raman spectra: a potential cancer diagnostic marker. Nano Lett. 2007; 7:1591-1597. [Crossref]
14. Lin JT. Analysis of the efficiency of photothermal and photodynamic cancer therapy via nanogolds and photosensitizers. J Cancer Research Update. 2017; 6:12-18. [Crossref]
15. Lin JT. Progress of medical lasers: fundamentals and applications. Med Devices Diagn Eng. 2016; 1:36-41. [Crossref]
16. Zhu TC, Finlay JC, Zhou X and Jun Li. Macroscopic Modeling of the singlet oxygen production during PDT. Proc SPIE Int Soc Opt Eng. 2007; 6427:6427O8. [Crossref]
17. Schumacher S, Mrochen M, Wernli J, Bueeler M and Seiler T. Optimization model for UV riboflavin corneal cross-linking. Invest Ophthalmol Vis Sci. 2012; 53: 762-769. [Crossref]
18. Kling S and Hafezi F. An algorithm to predict the biomechanical stiffening effect in corneal cross-linking. J Refract Surg. 2017; 33:128-136. [Crossref]
19. Lin JT and Cheng DC. Modeling the efficacy profiles of UV-light activated corneal collagen crosslinking. PloS One. 2017; 12:e0175002. [Crossref]
20. Lin JT. Photochemical Kinetic Modeling for Oxygen-enhanced UV-light-activated Corneal Collagen Crosslinking. Ophthalmoloy Research. 2017 (in press). [Crossref]
21. Wang S, Huang P, Nie L, Xing R, Dingbin Liu, Zhe Wang, et al. Single continuous wave laser induced photodynamic/plasmonic photothermal therapy using photosensitizer-functionalized gold nanostars. Adv Mater. 2013; 25:3055-3061. [Crossref]
22. Zhao X, Yuan Z, Yildirimer L, Zhao J, Lin ZY, Cao Z, e t al. Tumor-triggered controlled drug release from electrospun fibers using inorganic caps for inhibiting cancer relapse. Small. 2015; 11:4284-4291. [Crossref]
23. Zheng M, Zhao P, Luo Z, Gong P, Zheng C, Zhang P, et al. Robust ICG theranostic nanoparticles for folate targeted cancer imaging and highly effective photothermal therapy. Acs Appl Mater Interfaces. 2014; 6:6709-6716. [Crossref]
24. Zhang Z, Wang L, Wang J, Jiang X, Li X, Hu Z, et al. Mesoporous silica-coated gold nanorods as a light-mediated multifunctional theranostic platform for cancer treatment. Adv Mater. 2012; 24:1418-1423. [Crossref]
25. Liu Y, Zhi X, Meng Yang, Jingpu Zhang, Lingnan Lin, Xin Zhao, et al. Tumor-triggered drug release from calcium carbonate-encapsulated gold nanostars for near-infrared photodynamic/photothermal combination antitumor therapy. Theranostics. 2017; 7:1650-1662. [Crossref]
26. AbrahamseH and Hamblin MR. New photosensitizers for photodynamic therapy. Biochem J 2016; 473:347– 364. [Crossref]
27. Lucky SS, Idris NM, Li Z, Kai Huang, Khee Chee Soo and Yong Zhang. Titania coated upconversion nanoparticles for near-infrared light triggered photodynamic therapy. ACS Nano. 2015; 9:191–205. [Crossref]
28. Huang X. Giant enhancement of upconversion emission in NaYF4:Nd3+/Yb3+/ Ho3+)/(NaYF4:Nd3+/Yb3+ core/shell nanoparticles excited at 808 nm. Opt Lett. 2015; 40:3599–3602. [Crossref]
29. Yang Q, Zhao C, Zhao J and Ye Y. Synthesis and singlet oxygen activities of near infrared photosensitizers by conjugation with upconversion nanoparticles. Opt Mat Express. 2017; 7:913-923. [Crossref]
30. Lin JT, Chiang S, Lin GH et al. In vitro photothermal destruction of cancer cells using gold nanorods and pulsed-train near-infrared lase. J Nanomaterials. 2012; article ID 861385. [Crossref]
31. Lin JT, Hong YL and Chang C. Selective cancer therapy via IR-laser-excited gold nanorods. Proc SPIE. 2010; 7562. [Crossref]
32. Lin JT and Cheng DC. Optimal focusing and scaling law for uniform photo-polymerization in a thick medium using a focused UV laser. Polymers. 2014; 6:552-564. [Crossref]